M. AYAZ AHMAD,[1] MIR HASHIM RASOOL,[2] SHAFIQ AHMAD[2]

[1] Physics Department, Faculty of Science, Tabuk University
(P.O. Box 741, Saudi Arabia, K.S.A.; e-mail: mayaz.alig@gmail.com)
[2] Physics Department, Aligarh Muslim University
(Aligarh 202002, India; e-mail: sahmad2004amu@yahoo.co.in)

SCALING NATURE OF TARGET FRAGMENTS IN THE ^{28}Si-EMULSION INTERACTION AT AN ENERGY OF 14.6A GeV

PACS 25.75/-q

An attempt has been made to study the fractal behavior of the experimental data on nuclear fragments obtained from ^{28}Si-Emulsion collisions at 14.6A GeV. The whole analysis is performed by using two different methods, namely the methods of scaled factorial moments (SFMs), F_q, and multifractal moments, G_q. We have found that the present data reflect a multifractal geometry for nuclear fragments along with the Monte Carlo events (simulated events). Finally, some evidences of non-thermal phase transitions and the scaling law nature of SFMs have been studied.

K e y w o r d s: scaled factorial moments, multifractal moments, quark-gluon plasma, hadrons.

1. Introduction

The unusually large non-statistical particle density fluctuations in small phase space regions have attracted a lot of attention in the field of relativistic nuclear collisions to understand the mechanism of particle production. Several theoretical and experimental groups have suggested different methods to identify the existence of non-statistical fluctuations. Bialas and Peschanski [1] were the first to introduce the most suitable method known as the method of scaled factorial moments (SFMs) to study the non-statistical fluctuations in the distributions of relativistic shower particles produced in high-energy collisions. The proposal of these factorial moments was made in analogy with the phenomenon known as the intermittency in the hydrodynamics of turbulent fluid flows. On the other hand, R.C. Hwa and J.C. Pan [2] also first suggested a modified multifractal moments to extract the dynamical fluctuations in such heavy ion collisions. In high-energy physics, the power law behavior of the scaled factorial moment is known as the intermittency, where the power law behavior of a modified multifractal moment is known as the multifractality. One of the possible characteristics of the analysis of scaled factorial moments and modified multifractal moments is that it can detect and characterize the dynamical fluctuations, and it is also capable of filtering out the statistical noise. In these methods, the scaled factorial moments, F_q, and the modified multifractal moments, G_q, are computed as a function of the decreasing phase space size. The values of F_q and G_q for purely statistical fluctuations saturate with decreasing the phase space size, whereas F_q and G_q moments in dynamical fluctuations are supposed to increase with decreasing the phase-space size and exhibit a power law behavior of normalized factorial moments, F_q and G_q. However, the method of ordinary multiplicity moments ($\langle n^q\rangle/\langle n\rangle^q$) is used to demonstrate different features of multiplicity distributions and is unable to reveal the existence of dynamical fluctuations due to a significant contribution of purely statistical fluctuations.

The possibility of observing a new state of quark matter [3] has induced a lot of interest in the study of relativistic nucleus-nucleus collisions. The recent lattice QCD calculations [4] predict a phase transition of the nuclear matter of confined hadrons into a quark-gluon plasma (QGP) at a sufficiently high temperature (200–220 MeV), high energy density of the order of 3 GeV/fm^3, and/or high baryon density (>0.5/fm^3). It is widely believed that the strong interacting matter in these violent collisions undergoes a transition, temporarily, to a deconfined quark-gluon plasma (QGP). Initially, there was a strong speculation that the origin of intermittent-type non-statistical fluctuations was thought to be a result of the phase transitions from QGP to the normal hadronic matter in relativistic nucleus-nucleus collisions. But there is no experimental evidence for the formation of a quark-gluon plasma in low-energy nucleus-nucleus collisions. Further, no conclusive evidence of the formation of a quark-gluon plasma (QGP) has been found in nucleus-nucleus collisions at ultra-relativistic energies, and so on [5]. Therefore, the interpretation of the intermittency can no longer be related to the QGP formation. Only the future experiments would clarify the situation. It has been suggested that the Bose–Einstein (BE) interference [6] and the presence of a random cascade mechanism or short-range correlations may be responsible for the origin of the intermittency.

There is a strong feeling that the BE interference can play a role in dynamical fluctuations. This correlation arises due to the symmetric wave functions of identical bosons in the BE statistics. Increase in the value of factorial moments, F_q, with decreasing the phase-space size could be explained on the basis of the above correlations between identical charged particles. The phenomenon of intermittency would be stronger for identical charged particles than for all charged particles. Analysis of some experimental results [7–9] shows that the BE effect cannot be considered as the main source of the intermittency, especially in the $e^+ e^-$ annihilation [10] and lepton-hadron [11] and hadron-hadron collisions [12]. No such data are available for nuclear collisions. However, EMU01 data exclude the possibility of BE correlations as a dominant source of the intermittency in heavy ion collisions [13].

It has been observed that the intermittent behavior is clearly explained due to short–range correlations [13, 14] for a lower order of moments. The intermittency has also been observed in a variety of collision processes and, therefore, may be considered as a general property of the multiparticle production. However, no single mechanism could explain the observed intermittency in various collision processes. So, a detailed study is required to understand the intermittency more rigorously.

Till now, most of the works on dynamical fluctuations in high-energy nuclear collisions are carried out with a great interest in the produced shower particles, mostly pions, because it is assumed that these pions carry most of the information about the collision dynamics in the multiparticle production. However, only the little effort has been done to study the behavior of the intermittency and the multifractality of nuclear fragmentation processes. It is believed that, in high-energy nucleus-nucleus collisions, the emission of fast and slow target-associated particles takes place at a relatively later stage of the collisions. These fast protons known as grey particles in the energy range 30 to 400 MeV with relative velocity $0.3 \leq \beta \leq 0.7$ are quickly ejected initially, whereas slow protons and other heavier fragments with energies $\leq$30 MeV and relative velocity $\beta < 0.3$ are produced as a result of the evaporation processes. It is expected that these target-associated protons are believed to carry a relevant information about the dynamics of the emission process. Therefore, an attempt has been made to investigate the intermittent behavior and fractal properties of emission spectra of fast and slow target-associated particles from ^{28}Si-emulsion interactions at 14.6A GeV using a nuclear emulsion. It is also expected that such studies will not provide a unified description of the whole production processes, but such study may provide an additional parameter to understand the dynamics of the particle production process. In addition, the variations of the anomalous fractal dimensions, d_q, and the generalized dimensions, D_q, with the order of the moments, q, are investigated with the help of F_q and G_q moments. Some interesting conclusions regarding the multifractal specific heat and the occurrence of non-thermal phase transitions are presented.

2. Experimental Details

In the present experiment, FUJI nuclear emulsion pellicles were irradiated horizontally with a beam of

^{28}Si nuclei at 14.6A GeV at Alternating Gradient Synchrotron (AGS) of Brookhaven National Laboratory (BNL), New York, USA. The method of line scanning has been adopted to scan the stacks, which was carried out carefully using Japan-made NIKON (LABOPHOT and Tc-BIOPHOT) high-resolution microscopes with 8 cm movable stage using 40X objectives and 10X eyepieces by two independent observers, so that the bias in the detection, counting, and measurements can be minimized. The interactions due to beam tracks making an angle $<2^\circ$ to the mean direction and lying in the emulsion at depths >35 μm from either surface of the pellicles were included in the final statistics. The other relevant details about the present experiments and target identifications may be seen in our previous works [15–17].

2.1. Classification of tracks

All charged secondaries in these events were classified, in accordance with the emulsion terminology, into the following groups [15]:

2.1.1. b-Particles (black track producing particles):

Tracks with specific ionization $g^* > 10$ ($g^* = g/g_0$, where g_0 is the Plateau ionization of a relativistic singly charged particle and g is the ionization of the charged secondary) have been taken as black tracks. These correspond to protons with relative velocity $\beta < 0.3$ and range in emulsion $L < 3.0$ mm.

2.1.2. g-Particles (grey track producing particles):

Tracks with specific ionization $1.4 \leq g^* \leq 10$ corresponding to protons with velocity in the interval $0.3 \leq \beta \leq 0.7$ and range $L \geq 3.0$ mm in the nuclear emulsion are called grey tracks.

2.1.3. s-Particles (shower tracks producing particles):

Tracks with specific ionization $g^* < 1.4$ corresponding to protons with relative velocity $\beta > 0.7$ are classified as shower tracks. These tracks are mostly due to relativistic pions with small admixture of charged K-mesons and fast protons.

2.1.4. f-Particles (projectile spectator fragments):

Single and multiple charged ones emitted inside the fragmentation cone. Usually, we determine the number of alpha particles (n_α) and the number of fragments with $Z > 2$, separately.

2.2. Target mass and their identification

Nuclear emulsion detector is a heterogeneous mixture of Silver halide (AgBr), Gelatine (matrix material for the emulsion and a plasticizer, such as glycerin) and Water (H_2O). The chemical composition of the nuclear emulsion can be summarized as: 1% hydrogen (H), 16% Carbon-Nitrogen-Oxygen (CNO) and 83% Silver-Bromide (AgBr). The percentage of interactions in the emulsion with H, CNO or AgBr group of nuclei depends, however, on the energy and the identity of the incident beam. The average mass number, $\langle A \rangle$, of the different groups of nuclei may be obtained by the relation:

$$\langle A \rangle = \frac{\sum N_i A_i}{\sum N_i},$$

where N_i is the number of atoms per c.c. or mole per c.c. for the element of atomic number Z_i and atomic weight A_i. In the present experimental work, the values of mean target mass $\langle A \rangle$ equal to 1, 14, 70 and 94, respectively, for H, CNO, emulsion, and AgBr groups of nuclei.

2.2.1. Target Identification

The exact identification of a target in the emulsion experiment is not possible, since the medium of the emulsion is heterogeneous and composed of H, C, N, O, Ag, and Br nuclei. The events produced due to the collisions with different targets in the nuclear emulsion are usually classified into three main categories on the basis of the multiplicity of heavily ionizing tracks in it. Thus, the events with $N_h \leq 1$, $2 \leq N_h \leq 7$ and $N_h \geq 8$ are classified as collisions with hydrogen (H, $A_T = 1$), group of light nuclei (CNO, $\langle A_T \rangle = 14$), and group of heavy nuclei (AgBr, $\langle A_T \rangle = 94$), respectively.

However, the grouping of events only on the basis of N_h values does not lead to the right percentage of events of interactions due to the light and heavy groups of nuclei. In fact, a considerable fraction of stars with $N_h \leq 7$ are produced in the interactions with the heavy group of nuclei. Therefore, we have used the following criteria [15–17].

AgBr events:

(i) $N_h > 7$, or

(ii) $N_h \leq 7$ and at least one track with rang $R \leq 10$ μm and no track with $10 < R \leq 50$ μm.

CNO events:

(i) $2 \leq N_h \leq 7$ and no track with $R \leq 10$ μm.

H events:

(i) $N_h = 0$, or

(ii) $N_h = 1$, and no track with $R \leq 50$ μm.

3. Methodology Used

In order to get more information about the production mechanism in high-energy heavy-ion collisions, the multiplicity distributions of the produced particles were studied. If the production of particles takes place independently of each other, then the multiplicity distribution represents the Poisson distribution. On the contrary, if the production of a particle enhances the probability to produce other particles, then the multiplicity distribution is broader than the Poisson distribution, and its scaled factorial moments (SFMs) are larger than 1. The same thing should also happen for the multiplicity of particles produced in limited cells of the phase space. It is believed that the multiplicity fluctuations in small phase-space bins can reveal important aspects of the multiparticle production mechanism such as an intermittent pattern of fluctuations [1, 18, 19].

For the study of some worth mentioning informations about the non-statistical fluctuations in $\cos\theta$-distributions, of fast and slow target-associated particles in a given $\cos\theta$, the interval of total lengths $\Delta\cos\theta = \cos\theta_{\min} - \cos\theta_{\max}$, is divided into M bins of equal width, $\delta\cos\theta = \Delta\cos\theta/M$. Depending on the type of averaging, two types of moments are defined as:

(i) Horizontal Scaled Factorial Moments and
(ii) Vertical Scaled Factorial Moments.

3.1. Horizontal scaled factorial moments

Horizontal scaled factorial moments (SFMs) of different orders q are defined as [1, 20, 21]:

$$F_q^H = M^{q-1} \sum_{m=1}^{M} \frac{n_m\,(n_m-1)...(n_m-q+1)}{N(N-1)...(N-q+1)}, \quad (1)$$

where n_m is the number of grey or black tracks in bin m (m = 1, 2, 3, ...), and N represents the total multiplicity of grey or black particles in a particular event in the $\cos\theta$ intervals $\sim\Delta\cos\theta$.

For an ensemble of events of varying multiplicity, the above relation reduces to [22]

$$F_q^H = M^{q-1} \sum_{m=1}^{M} \frac{n_m\,(n_m-1)...(n_m-q+1)}{\langle N\rangle^q}, \quad (2)$$

where $\langle N\rangle$ represents the mean multiplicity of the grey or black tracks in the angular intervals $\sim\Delta\cos\theta = M\delta\cos\theta$.

On the averaging over the number of events in a data sample, one can get

$$\langle F_q^H\rangle = \frac{M^{q-1}}{N_{ev}} \times$$

$$\times \sum_{N_{ev}} \sum_{m=1}^{M} \frac{n_m\,(n_m-1)...(n_m-q+1)}{\langle N\rangle^q}. \quad (3)$$

It has been shown [1] that, for a smooth angular distribution of grey and black particles not exhibiting any fluctuations other than the statistical ones, $\langle F_q\rangle$ is essentially independent of the angular bin width $\delta\cos\theta$ in the limit $\delta\cos\theta \to 0$. However, if the fluctuations are dynamical in nature, then, in the limit a of small bin size, the scaled factorial moments [1] would obey the following power law:

$$\langle F_q^H\rangle = (M)^{\alpha_q} = \left[\frac{\Delta\cos\theta}{\delta\cos\theta}\right]^{\alpha_q} \text{ (for } \delta\cos \to 0). \quad (4)$$

The power-law dependence of the scaled factorial moments on the number of bins represented by the above relation is known as intermittency. The observation of such a power law may indicate a cascade mechanism of multiparticle production.

The power law predicts a characteristic linear rise of $\ln\langle F_q\rangle$ as a function of $\ln M$, which is represented by the relation

$$\ln\langle F_q^H\rangle = \alpha_q \ln M + C, \quad (5)$$

where α_q which measures the strength of intermittency is called the intermittency exponent, and C is a constant. The intermittency exponent, α_q, is obtained by performing the best fits according to Eq. (5):

$$\alpha_q = \frac{\Delta\ln\langle F_q^H\rangle}{\Delta\ln M}. \quad (6)$$

The scaled factorial moments are sensitive to the shape of the angular distribution. Thus, for a non-flat angular distributions varying within a finite bin of width $\delta\cos\theta$, one introduces an extra M-dependent correction factor, R_q, which is given by [23]

$$R_q = M^{q-1} \sum_{m=1}^{M} \frac{\langle n_m\rangle^q}{\langle n\rangle^q}, \quad (7)$$

where

$$\langle n_m \rangle = \frac{1}{N_{ev}} \sum_{i=1}^{N} \frac{\langle n_m, i \rangle^q}{\langle N \rangle^q}. \tag{8}$$

Thus, the corrected scaled factorial moments are calculated as

$$\langle F_q \rangle^{C\mathrm{corr}} = \frac{\langle F_q \rangle}{R_q}, \tag{9}$$

The correction factor R_q becomes, however, insignificant in the case of flat distributions.

The intermittency exponent, α_q, increases with the order of q of the moments. However, for a random uncorrelated particle production, $\langle F_q \rangle$ should be constant for all values of q showing the absence of non-statistical fluctuations. The power law behavior of the scaled factorial moments can also be interpreted in terms of fractal properties of the underlying physical process. Thus, it is possible to study a relation between the anomalous fractal dimensions, d_q, of fractals and multifractals in terms of intermittency exponents, α_q, with the help of the following relation [24]:

$$d_q = \frac{\alpha_q}{q-1}. \tag{10}$$

Independent values of the anomalous fractal dimension, d_q, for different q will show the existence of monofractality; whereas, in the case of multifractality, an order dependence of q is observed.

The power law behavior of $\langle F_q \rangle$ on M reveals the self-similarity. In general, this indicates the existence of fractal properties, which are called multifractals. According to the fractal theory, self-similar systems are characterized by the infinite spectrum of non-integer generalized dimensions, D_q. Therefore, the generalized dimensions, D_q that characterize multiparticle production process can be determined from the analysis of F_q-moments, using the relation

$$D_q = 1 - \frac{\alpha_q}{(q-1)}$$

or

$$D_q = 1 - d_q. \tag{11}$$

The monofractal structure of multiparticle spectra will show constant D_q values, which are associated with some collective phenomena (i.e., the formation of a quark-gluon plasma); whereas the multifractal structures are characterized by decreasing values of the generalized dimensions, D_q, with increasing the order of moments, q. The decreasing behavior of D_q with q is associated with a self-similar cascade process.

With the knowledge of Eqs. (5) and (6), we get firstly the values of intermittency index, α_q, which is the slope values of graphs plotted between $\ln\langle F_q \rangle^{\mathrm{corr}}$ Vs. $\ln M$ (More details in about the values of intermittency index, α_q, are discussed in Section 4.3). Thereafter, the possibility of detecting a non-thermal phase transition can be obtained by calculating the relevant parameter, λ_q, using the relation

$$\lambda_q = \frac{(\alpha_q + 1)}{q}. \tag{12}$$

3.2. Vertical scaled factorial moments

Another method known as the method of vertical scaled factorial moments, F_q^V, is suggested to correct for the non-uniform shape of the angular distribution, and it is also defined as

$$F_q^V = \frac{1}{M} \sum_{m=1}^{M} \frac{n_m(n_m-1)...(n_m-q+1)}{\langle n'_m \rangle^q}. \tag{13}$$

Performing the averaging over all the events, the vertical scaled factorial moments, $\langle F_q^V \rangle$, would become

$$\langle F_q^V \rangle = \frac{1}{N_{ev}} \sum_{i=1}^{N_{ev}} \frac{1}{M} \sum_{m=1}^{M} \frac{n_m(n_m-1)...(n_m-q+1)}{\langle n'_m \rangle^q}, \tag{14}$$

where $\langle n'_m \rangle = \frac{1}{N_{ev}} \sum\limits_{i=1}^{N_{ev}} n_m$, i is the average number of particles in the m^{th} bins for the entire data set having the number of events N_{ev}. The two definitions (3) and (14) become identical if the single-particle angular distribution is flat. However, if the distribution is not flat, one should either consider vertically averaged moments or apply a correction factor [23] to the horizontal moments.

3.3. Modified multifractal moments

Different methods have been used for studying the fractal nature of particles produced in a multiparticle production system at high-energy heavy ion collisions. R.C. Hwa, C.B. Chiu, and W. Florkowski [25,

26] proposed an approach in terms of multifractal moments, G_q, which can reveal the multifractal behavior of the particle spectra. But, for low multiplicity events, these multifractal moments are dominated by some statistical noise. Due to this fact, R.C. Hwa and J.C. Pan [2] first modified the old definition of multifractal moments, G_q, (old and modified, G_q, moments may be seen from our earlier publication [16 and references therein]) by introducing a step function which can act as a filter for the low-multiplicity events. The modified multifractal G_q-moments are used to minimize the contribution of statistical fluctuations.

4. Data Analysis and Outcomes

4.1. Variation of $\ln\langle F_q\rangle^{\rm corr}$ *with* $\ln M$

The whole $\cos\theta$-phase space has been divided into number of partitions M = 2–30, and the corrected scaled factorial moments $\langle F_q\rangle^{\rm corr}$ for the order of moments q =2–6 are calculated using Eq. (9) for grey and black tracks producing particles, respectively, in ^{28}Si-Em interactions at 14.6A GeV. The dependence $\ln\langle F_q\rangle^{\rm corr}$ on $\ln M$ is shown in Fig. 1, *a, b* in the $\cos\theta$-phase space for fast and slow target fragments. It is evident from the plots that the values of $\ln\langle F_q\rangle^{\rm corr}$ increase with $\ln M$ (i.e. decreasing the bin size). The linear rise in the values of $\ln\langle F_q\rangle^{\rm corr}$ with $\ln M$ with positive slope confirms the existence of the intermittency in the emission pattern of target-associated particles (i.e., grey and black). The observed increase in corrected factorial moments with decreasing the bin size clearly contradicts the evaporation model. The solid lines in Fig. 1, *a, b* represent the best-fitted line to data points. The errors shown in the above figures are estimated by considering them as independent statistical errors only, and the effects of correlation of statistical errors for different bin sizes have not been taken into consideration. The observation discussed readily confirms the signature of intermittency in the emission spectrum of fast and slow target associated particles. Similar results have been reported by other workers [27–29].

In order to check the presence of statistical fluctuations in the target fragmentation region, we have compared the experimental data with randomly generated uncorrelated Monte Carlo (MC-RAND) of 12,000 events. To see that the linear dependence of $\ln\langle F_q\rangle^{\rm corr}$ on $\ln M$ is not a spurious effect produced by the method itself, the uncorrelated MC events are

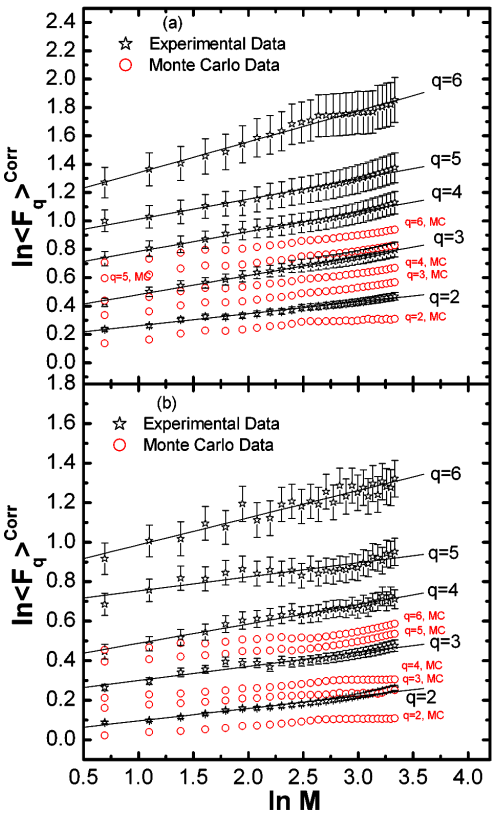

Fig. 1. Variations of $\ln\langle F_q\rangle^{\rm corr}$ as a function of $\ln M$ for grey particles (a) and black particles (b) in the cosθ phase space in ^{28}Si-Em collisions at 14.6A GeV along with the MC-RAND model

analyzed, and the results of this analysis are also depicted in Fig. 1, *a, b* by the red open circles with corresponding experimental data. It is observed that the experimental data exhibit the power law behavior, as expected. Monte Carlo generated events exhibit no such dependence on $\ln M$, i.e., show approximately a constant pattern. This gives an indication for the absence of the statistical contribution in the experimental data. The flat behavior in Monte Carlo events is expected for the independent emission of particles.

4.2. Behavior of $\ln\langle G_q\rangle$ *on* $\ln M$

In order to examine the dependence of $\ln\langle G_q\rangle$ on $\ln M$, the values of modified multifractal moments, $\langle G_q\rangle$ for q =2–6 have been calculated, using relation [2]

$$\langle G_q\rangle = 1/N_{ev}\left(\sum_{1}^{N_{ev}}\sum_{j=1}^{M}(n_j/N)^q * \theta(n_j - q)\right) \qquad (15)$$

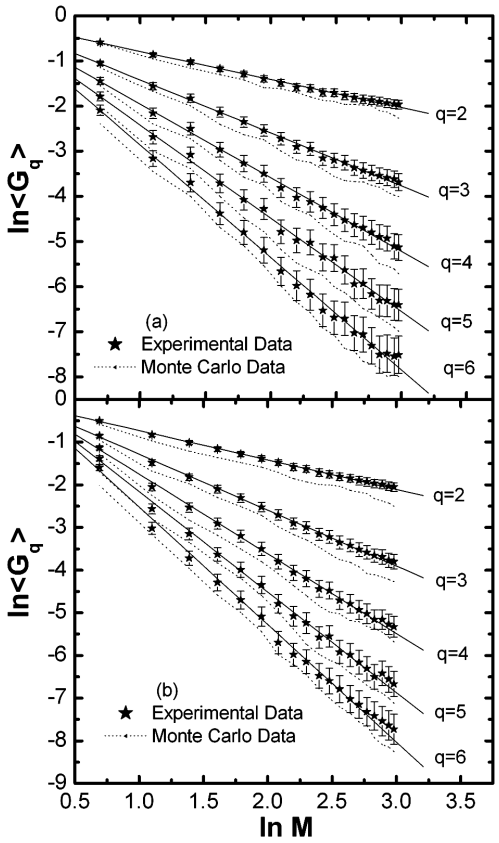

Fig. 2. Variations of $\ln\langle G_q\rangle$ as a function of $\ln M$ for grey particles (a) and black particles (b) in the cosθ phase space in ^{28}Si-Em collisions at 14.6A GeV along with the MC-RAND model

for fast and slow target associated particles in the $\cos\theta$ phase space for ^{28}Si-Em collisions at 14.6A GeV. The usual meaning of all input parameters in the above-mentioned relation is already defined in the earlier publication [2, 16]. The variations of $\ln\langle G_q\rangle$ as a function of $\ln M$ for grey and black particles are shown in Fig. 2, *a, b* for different q values in the $\cos\theta$ phase space. From these figures, a linear increasing trend is observed in the values of $\ln\langle G_q\rangle$ with a decreasing resolution of the bin width $\delta\cos\theta$ (i.e., increasing $\ln M$) for all values of q. The linear increasing pattern of the modified multifractal moments gives an indication of self-similarity for the mechanism of particle production in the target fragmentation region. Thus, the analysis of the present experimental work gives an initial indication of the fractal nature in the multiparticle production system. On the other hand, for the sake of comparison and/or to know the statistical contributions in the values of $\ln\langle G_q\rangle$, 10,000 events are generated in the $\cos\theta$ phase space using the uncorrelated Monte Carlo (MC-RAND) model with $\cos\theta$ values lying between –1 and +1. The values of $\ln\langle G_q\rangle$ with uncorrelated Monte Carlo (MC-RAND) have been also plotted in the same figures with $\ln M$. The generated events show a large deviation from experimental values for the higher order of moments, q, and are represented by dotted lines in the same figures for grey and black particles. Similar results have been represented in Gupta [30].

4.3. Nature of intermittency index, α_q, and mass exponent function, τ_q

The values of the intermittency index, α_q, obtained from the slopes of fitted solid lines in Fig. 1, *a, b* for various orders of factorial moments along with statistical errors for fast and slow target-associated particles are listed in Table 1. From the table, it is observed that the parameter, α_q, increases with the order of moments for grey and black particles. Further, it is also observed that the values of α_q, are slightly larger for the grey particles in comparison to those for the black particles for each value of q. Thus, it can be seen that the values of intermittency index, α_q, are also higher for highly energetic particles. Similar results have been reported by other workers [27]. It is evident from Table 1 that the values of intermittency indices α_q for our present data are slightly larger than the values of theoretical Monte Carlo data points, which reveal the predictions of the α-cascade model. The least square fitting of the experimental points in Fig. 2, *a, b* has been done to find the values of slopes, i.e., the mass exponent function, τ_q. The values of mass exponent function, τ_q, along with their statistical errors are also depicted in Table 2 for the order of moments q = 2–6. From this table, it is observed that the values of τ_q for both types of particles are found to be higher for the higher order of moments, q. The dependence of τ_q on the order of moments, q is shown in Fig. 3 for target-associated particles, i.e., grey and black particles, along with the values obtained by other workers [30]. It is also observed from the figure that the values of τ_q are nearly independent of the energy and the mass of projectiles, as well as of the target mass.

Table 1. **Values of intermittency index, α_q, obtained from least square fits of Eq. (5) for the experimental data**

Data set/Energy (A (GeV)	Tracks	α_2	α_3	α_4	α_5	α_6
^{28}Si-Em/14.6 Present	Grey	0.085 ± 0.004	0.184 ± 0.010	0.325 ± 0.017	0.513 ± 0.024	0.717 ± 0.035
M.C.– data Present	Grey	0.018 ± 0.004	0.024 ± 0.004	0.026 ± 0.005	0.027 ± 0.006	0.029 ± 0.006
^{28}Si-Em/14.6 Present	Black	0.042 ± 0.002	0.099 ± 0.006	0.162 ± 0.011	0.295 ± 0.023	0.436 ± 0.031
M.C.– data Present	Black	0.012 ± 0.002	0.015 ± 0.003	0.017 ± 0.002	0.020 ± 0.004	0.023 ± 0.005
^{16}O-AgBr/4.5 Ref. [27]	Grey	0.030 ± 0.002	0.101 ± 0.021	0.180 ± 0.047	–	–
^{16}O-AgBr/4.5 Ref. [27]	Black	0.009 ± 0.004	0.041 ± 0.017	0.094 ± 0.030	–	–

Table 2. **Values of mass exponent function, τ_q, obtained from least square fitting of graphs plotted between $\ln\langle G_q\rangle$ versus $\ln M$ to the experimental data**

Data set/Energy (A (GeV)	Tracks	τ_2	τ_3	τ_4	τ_5	τ_6
^{28}Si-Em/14.6 Present	Grey	0.622 ± 0.019	1.174 ± 0.035	1.628 ± 0.053	2.063 ± 0.065	2.491 ± 0.077
^{28}Si-Em/14.6 Present	Black	0.690 ± 0.016	1.319 ± 0.030	1.868 ± 0.040	2.356 ± 0.049	2.756 ± 0.059
^{84}Kr-AgBr/0.95 Ref. [30]	Grey	0.998 ± 0.023	1.384 ± 0.024	1.478 ± 0.053	–	–

4.4. Evidences from the anomalous fractal dimensions, d_q

The anomalous fractal dimension [31, 32], d_q, used for the description of fractal objects can be evaluated by Eq. (10). The formation of a quark-gluon plasma in thermodynamical equilibrium may be responsible for the production of a phase transition to the hadron phase [33]. If the phase transition is of second order, the hadrons in the final state would exhibit the intermittent behavior, and the anomalous fractal dimension, d_q, would be independent of the order of moments. On other hand, if the final-state hadrons are produced as a result of the cascading process, the anomalous fractal dimensions d_q would increase linearly with q. The variation of d_q with the order of moments q is shown in Fig. 4, *a, b* for grey and black particles produced in the interactions of ^{28}Si-Em collisions at 14.6A GeV using F_q and G_q moments, respectively. From the figures, it may be noted that the anomalous fractal dimension, d_q, obtained by both moments F_q and G_q, increases linearly with q, and this indicates the multifractal geometry of the emission spectra of target fragments. This analysis will be useful to understand the emission of target fragments, especially the emission of black particles. The present investigation shows a similar trend, as reported by other workers for different projectiles and different energies [27–29].

4.5. Behavior of generalized fractal dimension D_q vs. q

The power-law dependence of the scaled factorial moments and modified multifractal moments of the multiplicity distribution on the number of bins M reveals a self-similar behavior and indicates the multifractal structures. The generalized dimension D_q, a parameter of fractality, is calculated with the knowledge of Eqs. (11) for F_q and G_q moments [28] in the interactions of ^{28}Si-nucleus collisions at 14.6A GeV for grey

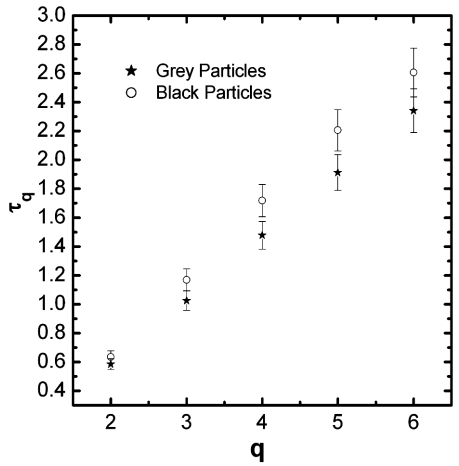

Fig. 3. Dependence of the mass exponent function, τ_q on the order of moments, q

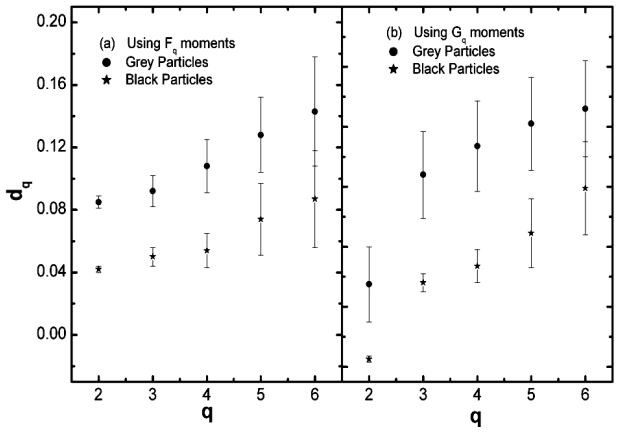

Fig. 4. Dependence of the anomalous fractal dimension, d_q on q for grey and black particles in ^{28}Si-Em collisions at 14.6A GeV for F_q moments (a) and G_q moments (b), respectively

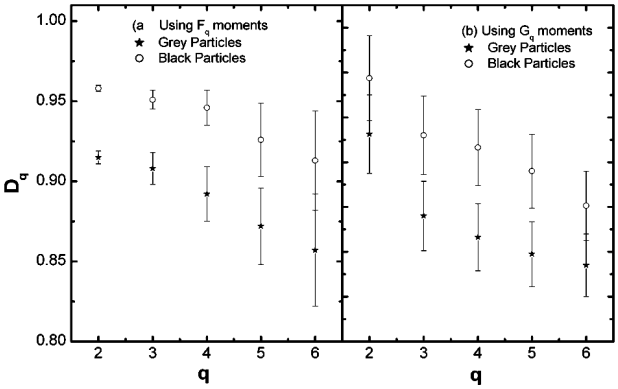

Fig. 5. Variation of the generalized fractal dimension D_q as a function of q for grey and black particles in ^{28}Si-Em collisions at 14.6A GeV for F_q moments (a) and G_q moments (b), respectively

and black particles. The values of D_q are plotted in Fig. 5, *a, b* as a function of the order of moments q in the $\cos\theta$-phase space for both moments F_q and G_q, respectively. It is obvious from the figures that the values of D_q decrease with the increasing the order of moments q for both types of particles. The analysis shows that the values of D_q are always less than 1 for all q for both moments F_q and G_q, as well as for both types of particles. The decreasing pattern in the values of D_q with the order of moments q clearly gives an agreement with the multifractal cascade mechanism [34], and this behavior also indicates that there is no existence of a second-order phase transition. These results are similar to those reported by other workers [27, 29, 30]. Therefore, the analysis of observed scaled factorial moments and G_q-moments reveals the self-similarity characteristic in the multiparticle production.

4.6. Multifractal specific heat

Recently, a multifractal Bernoulli distribution [35] was introduced to describe the transition from monofractality to multifractality, which is also believed to play a crucial role in the multiparticle production at high energies. This distribution is also used to find some systematic behavior in the experimental data on the fractal parameters of particles produced in heavy ion collisions. The multifractal Bernoulli functions satisfy the relation

$$D_q = D_\infty + c\,\ln(q/(q-1)), \tag{16}$$

where D_q is the generalized dimension of the order q, and c is a constant. The constant "c" in Eq. (15) can be interpreted as the multifractal specific heat of the system provided the thermodynamical interpretation of the multifractality is used [36]. It is widely believed in thermodynamics that the specific heat of gases and solids is constant and independent of the temperature [37] in a wide range of q. This analogy of the constant specific heat approximation should also be applicable to the multifractal specific heat.

In order to find the values of the multifractal specific heat, we have plotted the graph for the values of generalized fractal dimension, D_q, obtained from the analysis of F_q and G_q-moments against $\ln(q/(q-1))$ in Fig. 6, *a, b* for fast and slow target fragments produced in ^{28}Si-Em collisions at 14.6A GeV in the $\cos\theta$-phase space for F_q and G_q-moments. The straight lines shown in the above figure are best linear fits to the experimental points. One can see from the figures that the values of D_q reveal a linear increase as a function of $\ln(q/(q-1))$. The linear behavior in the figures indicates good agreement between the experimental data and the multifractal Bernoulli representation. The calculated values of multifractal specific heat extracted from the figures are shown in Table 3 for the present data corresponding to F_q and G_q-moments. There is no systematic variation in the values of multifractal heat "c" determined by the F_q and G_q-moments methods. The values of the multifractal specific heat found by two methods are

different. The obvious reason for this difference is due to different values of the generalized dimension, D_q, obtained in the analysis of two methods. This result does not reveal any kind of universality with respect to the various interactions.

4.7. Evidence of non-thermal phase transitions

It has been observed [31, 32] that if the dynamics of intermittency is due to the self-similar cascading, then there is a possibility of observing a non-thermal phase transition, which is believed to occur during the collision. If such a non-thermal phase transition is present, then function (12) should have a minimum at a certain value of $q = q_c$ [13]. The region with $q < q_c$ is dominated by numerous small fluctuations, whereas the region with $q > q_c$ is due to rarely large fluctuations. This situation can easily be compared with a mixture of the "liquid" of many small fluctuations and the "dust" consisting of few grains of very large density.

The "liquid" and the "dust" phases coexist. The variation of λ_q as a function of q for grey and black particles produced in ^{28}Si-Em interactions at 14.6A GeV has been shown in Fig. 7. The result of ^{16}O-AgBr at 4.5A GeV has also been shown for comparison. From the figure, it may be noted that no clear-cut minimum value of λ_q for a certain value of q has been observed in the present experimental work, as it is reported by other workers [38, 39]. However, a little deviation of the experimental data from the "no intermittency" line ($\alpha_q = 0$) indicates the presence of a weak intermittency effect in the $\cos\theta$-space for the present data. Thus, it may be concluded that the data for grey and black particles do not support a clear evidence for the existence of a non-thermal phase transition. To get a more unambiguous evidence, the analysis should be done up to $q = 8$ with large statistics at high energies and with different projectiles.

4.8. Scaling law nature of scaled factorial moments

Another consequence of the intermittency is a scaling property of SFMs in the multiparticle production. Seibert [40] proposed that higher-order scaled factorial moments, F_q, to the second-order factorial moments, F_2, are observed to obey the scaling law. The higher-order scaled factorial moments can be expressed in terms of second-order moments by the relation

$$(F_q - 1)/q(q-1) = (F_2 - 1)/2. \quad (17)$$

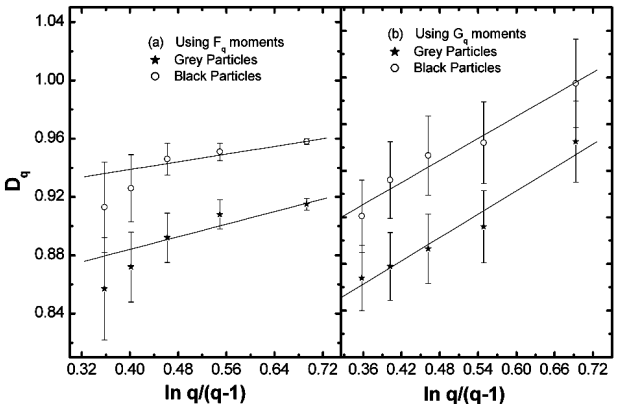

Fig. 6. Variation of D_q as a function of $(q/(q-1))$ for grey and black particles in ^{28}Si-Em collisions at 14.6A GeV for F_q moments (a) and G_q moments (b), respectively

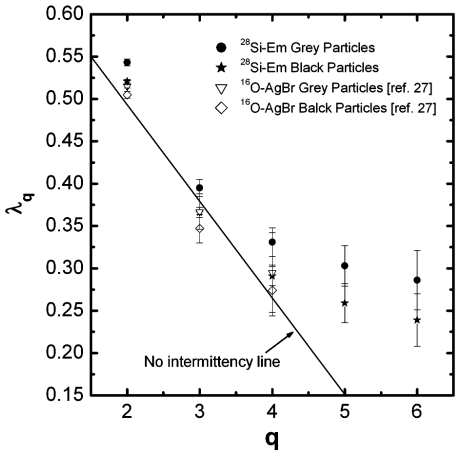

Fig. 7. Dependence of λ_q on the order of moments q in the $\cos\theta$ phase space for ^{28}Si-Em collisions at 14.6A GeV

Table 3. **Values of multifractal specific heat in the target fragmentation region of nuclear collisions**

Collisions/Energy (A GeV)	Particles	Using F_q moments	Using G_q moments
^{28}Si-Em/14.6 Present	Grey	0.108 ± 0.044	0.334 ± 0.120
^{28}Si-Em/14.6 Present	Black	0.085 ± 0.090	0.315 ± 0.132

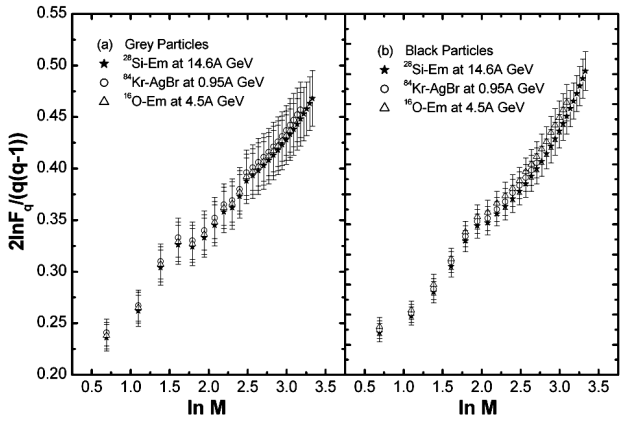

Fig. 8. Variation of $2\ln F_q(q/(q-1))$ as a function of $\ln M$ for grey and black particles in ^{28}Si-Em collisions 14.6A

Thus, the entire functional form of the q^{th}-order scaled factorial moments is determined by the second-order factorial moments. It has been reported [41] that, instead of expanding $(F_q - 1)$ as a function of $(F_2 - 1)\ln F_q$, it can also be expanded as a function of $\ln F_2$ toward the scaling law of F_q moments.

In order to check the validity of the above scaling law, the values of $2\ln F_q/q(q-1)$ for different values of q as a function of $\ln M$ are plotted in Fig. 8, *a, b* for grey and black particles in the $\cos\theta$-phase space. These figures also include the results obtained from the interactions of ^{16}O-AgBr and ^{84}Kr–AgBr collisions at energies of 4.5 and 0.95A GeV, respectively [27, 29]. It can be concluded that it favors the scaling behavior, but it is too early to say about the universality of the scaling law. To see the importance of the scaling nature, it would be interesting to further study the scaling law with different projectiles and energies.

5. Conclusion and Summary

On the basis of the above analysis, we may draw the following conclusions:

The observed increasing trend in the values of corrected factorial moments, F_q^{corr}, and modified G_q moments with decreasing the bin size clearly reflects the evaporation model and gives an evidence for an intermittency pattern of fluctuations in such heavy ion nucleus-nucleus collisions. The fractal behavior of the multiparticle production is observed for grey particles, as well as black particles, in the considered collisions of the target fragmentation region for the $\cos\theta$-phase space using F_q^{corr} and G_q moments. The values of intermittency indices, α_q, for experimental data are slightly larger than the values based on Monte Carlo data, which clearly reveals the predictions of the α-cascade model. The values of mass exponent function τ_q are found to be nearly independent of the energy and the mass of projectiles, as well as of the target mass. The anomalous fractal dimension, d_q, increases linearly with the order of corrected scaled factorial moments, F_q^{corr}, as well as modified multifractal moments, G_q, thereby indicating the multifractal geometry of the emission spectra of target fragments. This analysis is useful to understand the emission of target fragments, especially the emission of black particles. The decreasing trend in the values of the generalized dimensions, D_q with increasing the order of moments, q, obtained by F_q and G_q-moments indicates the possibility that the multiparticle production for grey and black particles is due to a self-similar cascade process. The different values of multifractal specific heat "c" determined by the $F_q$and G_q-moments method do not reveal any kind of universality with respect to the various interactions. Based on our study, we have not found any clear dip (clear-cut minimum) value of λ_q for a certain value of q. Thus, the given data on the target fragmentation do not show a clear indication for the occurrence of a non-thermal phase transition. Finally, a scaling behavior may be observed for higher-order scaled factorial moments (SFMs) in the present experimental data.

We would like to express our thanks and appreciation to Professor Gurmukh Singh, Department of Computer and Information Sciences, SUNY at Fredonia, Fredonia, NY 14063, U.S.A. for providing the exposed and developed nuclear emulsion plates/stacks. The author Dr. Mohammad Ayaz Ahmad also gratefully acknowledges that this work is supported in a part by the Deanship of Scientific Research of University of Tabuk/Ministry of Higher Education, Kingdom, Kingdom of Saudi Arabia with project No. S-1424-0035/15-02-1434.

1. A. Bialas and R. Peschanski, Nucl. Phys. B **273**, 703 (1986); Nucl. Phys. B **308**, 857 (1988).
2. R.C. Hwa and J.C. Pan, Phys. Rev. D **45**, 1476 (1992); R.C. Hwa, Phys. Rev. D **41**, 1456 (1990).
3. E.V. Shuryak, Phys. Rep. **115**, 151 (1984); E.V. Shuryak, Nucl. Phys. A **400** , 541 (1983).
4. E. Karsch, Z. Phys. C **38**, 147 (1988).

5. BRAHMS Collaboration. D. Rohrich *et al.*, J. Phys. G **31**, S659 (2005).
6. M. Gyulossy, Berkeley Preprint LBC-16831, 1989 (unpublished).
7. NA22 Collaboration. I.V. Ajinenko *et al.*, Phys. Lett. B **235**, 373 (1990).
8. TASSO Collaboration. W. Braunscheweig *et al.*, Phys. Lett. B **231**, 548 (1989).
9. I. Derado, G. Jancso, N. Schmitz, and P. Stopa, Z. Phys. C **54**, 357 (1992).
10. B. Buschbeck, R. Lipa, and R. Peschanski, Phys. Lett. B **215**, 788 (1988).
11. W. Shaoshun, Z. Jie, Y. Yunxiu, X. Chingua and Z. Yu, Phys. Rev. D **49**, 5787 (1994); UA1 Collaboration. C. Albajar *et al.*, Nucl. Phys. B **345**, 1 (1990).
12. NA22 Collaboration. I.V. Ajinenko *et al.*, Phys. Lett. B **222**, 306 (1989).
13. A. Capella, K. Fialkowski, and A. Krzywicki, Phys. Lett. B **230**, 149 (1989); P. Carruthers and I. Sarcevie, Phys. Rev. Lett. **63**, 1562 (1999); R.K. Shivpuri and V.K. Verma, Phys. Rev. D **47**, 123 (1993).
14. P. Carruthers, H.C. Eggers, and I. Sarcevie, Phys. Lett. B **254**, 258 (1991); P. Carruthers, Int. J. Mod Phys. A **4**, 5587 (1989).
15. M. Ayaz Ahmad and Shafiq Ahmad, Int. J. of Theor. and Appl. Phys. **2**, 199 (2012).
16. M. Ayaz Ahmad and Shafiq Ahmad, J. Phys. G: Nucl. Part. Phys. **32**, 1279 (2006).
17. M. Ayaz Ahmad and Shafiq Ahmad, Ukr. J. Phys. **2**, 1205 (2012).
18. B. Mandelbroat, J. Fluid Mech. **62**, 331 (1972).
19. U. Frisch, P. Sulem, and M. Melkin, J. Fluid Mech. **87**, 719 (1978).
20. B. Buschbeck, R. Lipa, and R. Peschanski, Phys. Lett. B **215**, 788 (1988); Phys. Lett. B **227**, 465 (1988).
21. W. Brauscheweig *et al.*, Phys. Lett. B **231**, 548 (1988).
22. A. Bialas and R. Peschanski, Jagellian University report JPJU/4/88.
23. K. Fialkowski and J. Woseik, Phys. Lett. B **214**, 617 (1988); Phys. Lett. B **232**, 76 (1989).
24. M. Dremin, Mod. Phys. Lett. A **3**, 1333 (1988).
25. R.C. Hwa and C.B. Chiu, Phys. Rev. D **43**, 100 (1991).
26. W. Florkowski and R.C. Hwa, Phys. Rev. D **43**, 1548 (1991).
27. Li Jun-Sheng, Liu Fu-Hu, and Zhang Dong-Hai, Chin. Phys. Lett. V **24**, 2789 (2007).
28. Dipak Ghosh *et al.*, Nucl. Phys. A **720**, 419 (2003).
29. B. Bhattacharjee, Nucl. Phys. A **748** 641 (2005).
30. B. Bhattacharjee and S. Sen Gupta, Int. I. Mod. Phys. E **14**, 1223 (2005).
31. A. Bialas and K. Zalewski, Phys. Lett. B **238**, 413 (1990); A. Bialas and K. Zalewski, Nucl. Phys. B **237,** 65 (1989).
32. B. Buschbeck, R. Lipa, and R. Peschanski, Phys. Lett. B **215,** 788 (1988); B. Buschbeck, R. Lipa, and R. Peschanski, Phys. Lett. B **227,** 465 (1988).
33. A. Bialas and R.C. Hwa, Phys. Lett. B **253**, 436 (1991).
34. C. Meneveau and K.R. Sreenivasan, Phys. Lett. **59**, 1474 (1987); R. Hasan *et al.*, Fractals **25**, 1029 (2005); D. Ghosh *et al.*, Fractals **11**, 331 (2003); Nucl. Phys. A **707**, 213 (2002).
35. A. Bershadskii, Phys. Rev. C **59**, 364 (1999).
36. E. Stanely and P. Meakin, Nature **335**, 405 (1988).
37. L.D. Landau and E.M. Lifshitz, Phys. Z. Sowjet **6**, 244 (1934).
38. D. Ghosh *et al.*, Fractals **11** , 331 (2003); D. Ghosh *et al.*, Z. Phys. C **71**, 243 (1996).
39. E.A. De Wolf, I. Dremin, and W. Kittel, Phys. Rep. **270**, 1 (1996).
40. D. Seibert, Phys. Rev. D **41**, 3381 (1990).
41. M. Ayaz Ahmad *et al.*, Indian J. of Phys. **84**, 12, 1675 (2010), DOI: 10.1007/s12648-010-0156-2.

Received 16.12.12

М. Аяз Ахмад, Мір Хашим Расул, Шафід Ахмад

СКЕЙЛІНГОВА ПРИРОДА
ФРАГМЕНТІВ МІШЕНІ ПРИ ВЗАЄМОДІЇ
^{28}Si З ЕМУЛЬСІЄЮ ПРИ ЕНЕРГІЇ 14,6*A* ГеВ

Р е з ю м е

Вивчено фрактальну поведінку експериментальних даних по ядерних фрагментах, отриманих в зіткненнях ^{28}Si з емульсією при 14,6*A* ГеВ. Весь аналіз виконано з використанням двох різних методів: масштабованих факторіал-моментів F_q і мультифрактальних G_q моментів. Ми виявили, що дані вказують на мультифрактальну геометрію для ядерних фрагментів разом з Монте-Карло подіями (моделювання подій). Крім того, вивчено деякі свідчення про нетеплові фазові переходи і природу закону подібності для масштабованих факторіал-моментів.